Journal of Materials Chemistry A

Accepted Manuscript

ROYAL SOCIETY OF CHEMISTRY

www.rsc.org/materialsA

Polarization induced dynamic photoluminescence in carbon quantum dot-based ionic fluid†

Lopamudra Bhattacharjee,[a] Kallol Mohanta,[a] Kaushik Pal,[b] Apurba L. Koner,[b] and Rama Ranjan Bhattacharjee[a]*

Abstract

We have recently reported the synthesis of water-dispersible, polymer-passivated and redox-active carbon quantum dots (CQDs). The CQDs were converted into a solvent-less conductive fluid through a step-wise surface modification technique. The material has a core-corona-canopy structure with CQD as core, passivating-polymer as corona and polyetheramine (Jeffamine®) as canopy. These materials are unique in characteristics and are designated as nano-ionic materials (NIMs). Structure and properties of CQD-NIMs were determined with dynamic light scattering, thermogravimetry, differential scanning calorimetry, photoluminescence (PL) and cyclic voltammetry (CV). Dynamic changes in extrinsic PL maxima (λ_{em}) of the CQDs were observed during and after CV. Such fluctuations in λ_{em} helped to understand the sequential ordering and disordering of Jeffamine® canopy on the CQD surface during polarization during CV. The phenomenon enables us to understand molecular canopy dynamics in NIMs and further showcase redox-active CQDs as a sustainable material for future electrochemical applications.

Introduction

Functional nanomaterials are currently at the forefront of materials research. Surface passivation and functionalization of nanomaterials enable control over their physicochemical properties and enhance their multidirectional applicability. The surface structure in these materials plays a vital role in predicting the way these systems function. One such interesting structure is the core-corona-canopy design in fluid-like nano-ionic materials (NIMs). First introduced by Giannelis and coworkers, these functional nanomaterials show interesting rheological properties.[1,2] Literature suggests that the fluidic properties are tunable with variations in the type of core-corona and nature of chosen canopy.[3-5] We had earlier reported surface-modification of gold nanorod (GNR) corona with a Jeffamine® canopy through electrostatic self-assembly, that resulted in a plasmonic fluid.[3] Shear induced dynamic changes in plasmonic characteristics of GNRs were monitored and attributed to the Jeffamine® canopy induced slow relaxation/rearrangement of the GNRs assemblies.[3] Dynamics of the canopy determine the fluidic property in NIMs and can be probed using rheological, neutron scattering and NMR techniques.[1-6] The results obtained from NMR and rheological studies indicated that the liquid-like behavior in NIMs is due to the rapid exchange of canopy between the ionically-modified nanoparticles used as core materials.[6] Among various core materials reported so far, few carbon-based core materials have been used for NIMs studies. Giannelis *et al.* have reported synthesis of NIMs by neutralizing fully protonated fullerol with an amine terminated polyetheramine that exhibited complex viscoelastic behavior.[4] Graphene oxide quantum dots have been modified into a fluid by Zhang *et al*. that exhibited excellent solubility and amphiphilicity.[5]

Carbon quantum dots (CQDs) are a new class of interesting carbon based nanostructures that can be produced from various carbon resources.[7-12] The main challenge for chemists is to

tune the structure of the CQDs by controlling the density of sp^2 islands in the sp^3 matrix.[12,13] CQDs have consistently gained interests due to their non toxic nature, unique photoluminescence[12-14] (PL) and conducting properties.[15,16] Wen *et al*. reported that the PL of CQDs consists of two spectral bands. These bands are termed intrinsic and extrinsic bands and corresponds to band gap and surface trap states respectively.[12-14] The bands can be tuned by tuning the size of sp^2 nano-domains and mode of preparation of the CQDs.[17,18] The highly emitting CQDs have been increasingly utilized in bio-imaging[19-21] as well as in designing light emitting diodes (LEDs).[22] Among other important applications, CQDs have been coupled with materials like TiO_2 and RuO_2 for applications in supercapacitors and efficient electrodes for batteries.[23-26]

Recently we have reported conducting PSS-CQDs which were prepared in a single step pyrolysis of citric acid and Poly (sodium 4-styrene sulfonate) (PSS) mixture. The PSS-CQDs showed stable redox behavior within an appreciable voltage regime.[27] In the present manuscript, we have used step-wise surface modification technique to convert powdered PSS-CQDs into CQD-NIMs at room temperature. The CQD-NIMs consisted of redox active CQDs [27] as core and Jeffamine® as canopy (Scheme 1). The redox active CQD-NIMs sample was used as an electrolyte and its CV properties were studied. Interestingly, it was observed that the extrinsic PL maxima (λ_{em}) of CQD-NIMs dynamically shift during and after CV cycles. The phenomenon was studied in details and reasons for the dynamic λ_{em} behavior under CV induced polarization were predicted. The work may provide a PL based approach towards understanding molecular canopy dynamics in NIMs-like fluids. The use of redox-active-CQDs has been showcased as an effective core material in NIMs-class of materials that can be used in future electrochemical applications.

Experimental

Materials: Citric acid (99.7%) was purchased from Himedia Chemicals. Poly (sodium 4-styrene sulfonate) (99.8%, M.W. 70,000) (PSS) was purchased from Sigma-Aldrich and it was used as received without further purification. Jeffamine® (M2070) was obtained as gifted sample from Huntsman (India). DOWEX® HCR-W2-hydrogen resin was purchased from Sigma-Aldrich. Dialysis membranes were purchased from Himedia. Milli-Q water was used in all experiments. All the measurements were performed at room temperature (*ca.* 25ºC) unless otherwise mentioned.

Method of preparation of CQD-NIMs:

PSS-passivated CQDs (PSS-CQD) were prepared in one step pyrolysis method using citric acid and PSS as precursors. The process was adopted form our previously reported work.[27]

Ion exchange and surface modification of CQDs

The ion exchange process to modify CQDs was done with slight modifications following our earlier reported method on the designing of gold nanorod-based NIMs.[3] We have performed ion exchange in CQDs and modification of the ion exchanged product was done with Jeffamine®. A column was prepared with Dowex HCR-W2 Hydrogen resin. Before charging in column, resin was washed several times with Milli-Q water. For the preparation of CQD-NIMS, 0.5g PSS-CQD was dispersed in 150 ml Milli-Q water. The suspension was dialyzed by HIMEDIA-110 dialysis membrane in Milli-Q water for 24 h and passed through resin packed column. The ion-exchange process was repeated three times to ensure that Na^+ ions present in CQDs get completely replaced by H^+ ions. The eluate showed pH value 2.6. It was collected from the column and titrated with 0.1M aqueous Jeffamine® solution. Final pH of the suspension was recorded to be 3.5. Similarly two other CQD-NIMs were prepared at different pH (pH 4.5 &

5.1). The Jeffamine® content increases with increase in pH. Suspension was freeze-dryed and CQD-NIMS was obtained as brown liquid. The liquid was further dried and degased in vacuum desiccator. Final products were solvent free and liquid at room temperature. CV studies indicated that CQD-NIMs prepared at pH 3.5 shows redox properties.

Equipments and characterization techniques

Dynamic Light Scattering (DLS) was performed with Zetasizer from Malvern. Thermal degradation of CQDs-NIMs were studied by thermogravimetry (TGA) using a NETZSCH STA 449 F3 Jupiter thermal analyzer. PL data were recorded by Shimadzu RF5301 Fluorimeter. All the steady state steady state measurements were carried out using HORIBA Jobin Yvon Fluorimax-4 Fluorimeter. PL spectra of CQD-NIMS were recorded upon excitation at 420 nm using slit width of 3 nm. The corresponding emission maxima (λ_{em}) were recorded in the regime of 450-500 nm. Life-time studies indicated the emission band ~ 500 nm has a life-time ~ 3.9 ns as shown in Electronic Supplementary Information (ESI)† (Fig. ESI1). This band must correspond to the λ_{em} as reported by Wen *et al.*[14] λ_{em} with large bandwidth originates from the surface sates present in CQDs and which is well documented in literature. During CV cycles, the surface of the CQDs is polarized due to changes in polarity of the surface environment, *i.e.*, changes in conformation of the Jeffamine® canopy. Hence to understand the phenomenon with fluorescence, we decided to measure the λ_{em}. λ_{em} was recorded immediately before and after CV experiment with solid state accessories.The CQD-NIMS fluid was collected from the CV workstation and drop coated on spectroscopic grade quartz plate. The same was placed inside the solid-state accessory of the spectrofluorometer. A differential scanning calorimetry (DSC) device (Pyris Diamond DSC, Perkin−Elmer) was used to study the glass-transition temperatures (T_g) of the CQD-NIMs. Samples were kept at 50 °C for 30 min under isothermal conditions and scanned

from 50 °C to 100 °C at a heating rate of 10 °C/min, then cooled to -100 °C. Two cycles were performed. The DSC equipment was calibrated using In and Zn as calibration materials prior to scanning the samples.

Cyclic Voltammetry: CV experiments were done by CH instruments (CHI 600E) Austin, Texas. Before electrochemical measurements at metallic electrode, CQD-NIMS fluid was degassed and dried under vacuum for few days so that no traces of water or oxygen remain within the fluid. For electrochemical measurements at a Pt electrode, CQD-NIMS was transferred to an air tight glass cell (φ25 mm × 40 mm) with a teflon cap (φ300 mm). A three electrode system was used where Pt was taken as working electrode (metal disk encapsulated by kel-Fφ 6.35mm) and Pt-wire (φ 0.5mm) and Ag/AgCl were used as counter and reference electrode respectively.

Results and discussions

The CQD-NIMs was designed by a resin-exchange process followed by simple acid-base titration as detailed in experimental section.[3] During titration, the surface -SO_3H groups on CQDs exchange proton with the terminal amine group of Jeffamine® creating an anionic corona and a cationic canopy as shown in Scheme 1.[3] DLS of CQD-NIMS was obtained after dialyzing the samples with HIMEDIA-110 dialysis membrane followed by filtration with 0.22 μm cellulose nitrate membrane. Intensity average hydrodynamic radius of CQD-NIMs shows two peaks at ~10.5 nm and 32.8 nm respectively (Fig. 1A). The first peak (10.5 nm) is due to individual CQDs and is in agreement with the size of CQDs observed in TEM images.[27] The second peak at 32.8 nm may be due to canopy formation by Jeffamine® around PSS-CQDs. Multiple particles can also form cores leading to different sizes of core-corona-canopy structures and thus multiple peaks may be detected.[3] Lower negative zeta potential value (-10.4 mV) of

CQD-NIMs (Fig. 1B) together with a tailing towards positive zeta region indicate surface charge neutralization in presence of cationic Jeffamine® on PSS-CQDs surface. From DLS it is apparent that there is a core CQD which might be surrounded by polymer canopy as shown in Scheme 1.

The CQD-NIMs showed enhanced solubility in a wide range of solvents as shown in Fig. ESI2. The enhanced solubility can be attributed to the amphiphilic nature of Jeffamine® as canopy. Similar observations have been reported for fullerol and graphene oxide based NIMs.[4,5] Presence of Jeffamine® was evident in TGA thermogram. TGA of CQD-NIMS (Fig. 1C) shows 96.6% mass loss at ~ 407 ºC which is due to degradation of Jeffamine® canopy attached to the core CQDs through electrostatic interactions with the PSS corona. At around 300 ºC, a small change in mass was observed which might be due to degradation of PSS attached with CQDs (~3%).[27] CQDs-NIMs have fluid-like appearance of at room temperature. DSC thermogram (Fig. 1D) shows T_g of the CQD-NIMs ~ - 50 °C. The value is lower than room temperature and hence the material is liquid at room temperature. The T_g value of pure Jeffamine® is ~ - 71°C.[4] The increase in T_g value of CQD-NIMs compared to that of pure polymer indicates formation of core-canopy structure. Similar observation has been reported for fullerol based NIMs.[3]

CQD-NIMs fluid was taken as electrolyte for CV experiment and no additional electrolyte was added. The starting potential was -3.0 V. It was scanned till the switch potential point of +3.0 V and swiped back to end potential at -3.0 V. The fluid was stable in the voltage regime of 6V. The scan rate was kept fixed at 50 mV/s. PL spectra recorded upon excitation at 420 nm before and after CV experiments, showed red-shift in λ_{em} (inset in Fig. 2). PL spectra of CQD-NIMs recorded before CV shows λ_{em} at 494 nm, that red-shifted to 506 nm after 5 CV cycles (inset in Fig. 2). Different numbers of CV cycles were performed and λ_{em} was recorded immediately after completion of each run. λ_{em} was plotted with number of cycles as shown in

Fig. 2. The plot indicated no red-shift beyond 5 cycles. Interestingly, λ_{em} was observed to gradually blue-shift with time as evident from time dependant studies performed after 10 CV cycles (Fig. 3). After ~ 2 h, λ_{em} was observed at 494 nm, which was the original λ_{em} before CV.

Spectral changes observed for λ_{em} (Fig. 2&3) of CQDs-NIMs can be related to dynamic changes in surface environment under polarization. Initially, the Jeffamine® matrix embedding the CQDs, remain un-polarized (Scheme 1). The free electrons of CQDs populate the surface trap states (STS) at room temperature.[27] During forward scan in CV (Oxidation), electron transfers from the STS of CQDs to +ve electrode as shown in Scheme 2. In the reverse scan (Reduction), electron transfers from –ve electrode to LUMO of the CQDs. After CV (Relaxation), electrons from LUMO can get transferred to Jeffamine® canopy through STS as shown in Scheme 2. This is possible as the Jeffamine® canopy in the CQD-NIMs is cationic and hence electron deficient. Electron donation to the Jeffamine® canopy partially polarizes CQD-NIMs structure thus creating a compact canopy (Scheme 2). Formation of a compact cationic Jeffamine® canopy around the anionic CQDs passivated PSS core-corona structure can lower the energy of the STS (Scheme 2). The situation is similar to the lowering of excited energy state of a molecule due to changes in polarity of solvent molecules in solution.[28] The lowering in energy of the STS is evident in the red-shift of λ_{em} of the CQDs after CV cycles (Fig. 2). Extent of polarization of canopy increases with increase in number of CV cycles. Such polarization strengthens the cationic Jeffamine® canopy resulting in further stabilization of STS present on the core CQDs (Scheme 2). The stabilization leads to gradual red shift in λ_{em} as indicated in Fig. 2. λ_{em} values acquire a limiting value after 5 cycles indicating attainment of maximum polarization and absolute compactness of the corona-canopy structure as shown in Scheme 2. The relaxation dynamics of the corona-canopy structure of CQD-NIMs can be visualized through

time dependant blue-shift of λ_{em} as shown in Fig. 3. Considering, that the cationic Jeffamine® canopy is dynamic and it moves from one anionic CQD to another, we can predict that the polarized structure of the Jeffamine® canopy relaxes once CV is turned off.[6] The relaxation is driven by the laws of thermodynamics. During polarization, the ordering of canopy around the CQD corona decreases the entropy of the system. In order to gain entropy, that is to create the random/un-polarized state, the systems relax back to its original conformation (Scheme 1). The randomness in the Jeffamine® canopy structure remove its stabilizing affect on the surface trap state of CQDs. Consecutively, the energy of surface trap states of CQDs increases as indicated by the gradual blue-shift in extrinsic λ_{em} values (Fig. 3). The changes in energy of the surface trap states due to dynamic changes in surface environment of CQDs result in only minute changes in λ_{em} values (from 494 to 505 nm). The shifts in λ_{em} values with minute changes in polarity in the immediate vicinity of the CQD surface can be observed upon exposure of the CQD-NIMs to different solvents. Thus λ_{em} values for water and ethanol were observed at 445 and 455 nm respectively. The effect of solvent dielectric constant on λ_{em} is well reported in literature.[28]

CV data obtained from first cycle shows the oxidation and reduction peaks at -0.83 V and +1.0 V respectively (Fig. 4). The peaks appear due to redox process of the CQDs.[27] Such saturating nature of the CV curve indicates that the to & fro electron transfer process between CQDs and electrodes is quite fast. It is also noticed that unlike CV of aqueous CQD,[27] the current here is constantly increasing with potential, making a "paunch" or a window in CV spectra (Fig. 4). This can be attributed to the interactions of negatively charged CQDs with cationic Jeffamine® canopy through electrostatic interactions.[29,30] Due to this interaction and surrounding insulating Jeffamine® matrix, there is consistent flow of charges through the

electrolyte (CQD-NIMs). Nevertheless, within this paunch area i.e. from -1.0 V to +2.5 V, which has been created due to reduction of CQDs, the material can pile up enough charge carriers.[31] CV characterization of only Jeffamine® shows no significant redox properties (Fig. ESI3). CQD-NIMs samples prepared at higher Jeffamine® contents did not show redox behavior. This may be due to greater concentrations of insulating Jeffamine® present in those systems.

Interestingly, though CV experiments revealed the presence of oxidation peak at 1.0 V during the first scan, further cycles showed oxidation at 1.4 V that deviate slightly in further cycles (Fig. 4 & ESI 4). When CV was run after a delay, the first scan showed the oxidation peak position to be back at 1.0 V. Such increase in oxidation potential is related to stabilization of surface trap states in CQDs during polarization of the Jeffamine® canopy.[13,7] During forward scan in CV (Oxidation), Jeffamine® polarizes near the CQD surface (Scheme 2). The compact canopy result in stabilization of the surface trap states in CQDs.[32,33] Decrease in energy level creates hindrance for electron transfer from CQDs to +ve electrode surface in the consecutive CV cycles. Hence the increase in oxidation potential after the first cycle (1 to 1.4 V) was observed (Fig. 4). In consecutive cycles, the canopy structure is further reinforced which results in slight higher energy shift of the oxidation peak in consecutive CV cycles as shown in Fig. ESI4. After 10 cycles, there was no further shift in oxidation peak position (Fig. ESI4). Once CV is switched off and the CQD-NIMs was allowed to relax, the original surface energy states are repopulated (peak at lower voltage 1.0 V is observed).[30] The slight increase in life-time of the CQD-NIMs after different CV cycles (Fig. ESI1) indicate decrease in radiative decay rate due to stabilization of surface trap states as a function of polarization. The same is in line with the red-shift of extrinsic emission maxima with increasing CV cycles as observed in the manuscript.

Thus both PL and CV results reinforce the fact that dynamic changes in canopy structure under polarization influence surface trap states of core CQDs in the CQD-NIMs fluid.

In conclusion, we have shown that the extrinsic PL band (λ_{em}) of CQD-NIMs shows spontaneous and reversible fluctuations (blue shift & red shift) under polarization. Though the red shift is only 12 nm (494 to 506 nm after 10 consecutive CV cycles), it is of immense importance. There was neither any change in solvent polarity nor any ligand exchange processes on the surface of CQDs. The red-shift can only be interpreted by considering ordering and disordering of Jeffamine® canopy on the immediate vicinity of the CQD surface in the NIMs material. The canopy dynamics influenced fluctuations in surface trap states of CQDs. This was proved from CV data of CQD-NIMs obtained from multiple cycles. Finally, λ_{em} was shown to be used for monitoring the molecular canopy dynamics of NIMs. The simplicity of the method allows realization of the canopy dynamics through PL approach and can be helpful to prepare green electrolyte material for future battery applications.

Acknowledgements

The work was funded by the Department of Science & Technology (New Delhi) (SR/FT/CS-128/2010). LB thanks Ministry of Earth Sciences (MoES/P.O.(Seismo)/1(190)/2013) for support and fellowship. Support from PSG Institute of Advanced Studies is gratefully acknowledged. We thank Prof. Tushar Jana (Central University Hyderabad, India) for DSC experiments. Finally we thank HUNTSMAN (India) for providing the Jeffamine® polymer as gift sample.

Notes and references:

[a] **PSG Institute of Advanced Studies, Coimbatore, Tamil Nadu, 641004, India. Tel: +91-422-434-4000, Fax: +91-422 257-3833 E-mail: ramaranjanb89@gmail.com (Dr. Rama R. Bhattacharjee)*

[b] *Department of Chemistry, Indian Institute of Science Education & Research Bhopal, Bhopal By Pass Road, Bhauri, Bhopal, 462066, India. Tel:+91-755-669-2376, Fax: +91-755-669-2392*

† *Supporting Information available: [Life-time measurements, Solubility results, CV of pure Jeffamine® and CV of 10 consecutive cycles for CQD-NIMs].*

References:

1. R. Rodriguez, R.Herrera, L. A. Archer, E. P. Giannelis, *Adv Mater*., 2008 ,**20**, 4353.
2. A. B. Bourlinos, S. R. Chowdhury, R. Herrera, D. D. Jiang, Q. Zhang, L. A. Archer, E. P. Giannelis, *Adv. Funct. Mater.,*2005, **15**, 1285.
3. R. R.Bhattacharjee, R. Li, L. Estevez, D-M. Smilgies, A. Amassian, E. P. Giannelis *J. Mater. Chem.,* 2009, **19**, 8728.
4. N. Fernandes, P. Dallas, R. Rodriguez, A. B. Bourlinos,V. Georgakilas, E. P. Giannelis, *Nanoscale*, 2010, **2**, 1653.
5. C. Zeng, Z.Tang, B.Guo, L. Zhang, *Phys. Chem. Chem. Phys.,* 2012, **14**, 9838.
6. M. L. Jespersen, P. A. Mirau, E. von Meerwall, R. A. Vaia, R. Rodriguez, E. P.Giannelis, *Nanoscale*, 2010, **4**, 3735.
7. A. B. Bourlinos, A. Stassinopoulos, D. Anglos, R. Zboril, M. Karakassides, E. P. Giannelis, *Small*, 2008, **4**, 455.
8. J. Wang, C. F. Wang and S. Chen, *Angew. Chem., Int. Ed.,* 2012, **51**, 1.

9. Y.-P. Sun, B. Zhou, Y. Lin, W. Wang, K. A. S. Fernando, P. Pathak, B. A. Harruff, X. Wang, H. Wang, P. G. Luo, H. Yang, B. Chen, L. M. Veca and S.-Y. Xie, *J. Am. Chem.Soc.,* 2006, **128**, 7756.
10. L. Cao, X. Wang, M. J. Meziani, F. Lu, H. Wang, P. G. Luo, Y. Lin, B. A. Harruff, L. M. Veca, D. Murray, S.-Y. Xie, Y.-P. Sun, *J. Am. Chem. Soc*., 2007, **129**, 11318.
11. F. Liu, M.-H. Jang, H. D. Ha, J.-H. Kim, Y.-H. Cho, T. S. Seo, *Adv. Mater*., 2013, **25**, 3657.
12. P. Yu, X. Wen, Y.-R. Toh, J. Tang, *J. Phys. Chem. C*, 2012, **116**, 25552.
13. L. Cao, M. J. Meziani, S. Sahu, Y. P. Sun, *Acc. Chem. Res*., 2013, **46**, 171.
14. X. Wen , P. Yu , Yon-Rui Toh , X. Hao , J. Tang , *Adv. Optical Mater.* 2013, **1**, 173.
15. S. Mondal, U. Rana, S. Malik, *Chem. Commun.*, 2015,**51**, 12365.
16. J. Wang, C. F. Wang, S. Chen, *Angew. Chem. Int. Ed*., 2012, **51**, 1.
17. Y. Wang, A. Hu, *J. Mater. Chem. C*, 2014, **2**, 6921.
18. H. Li, Z. Kang, Y. Liu, S-T, Lee, *J. Mater. Chem*, 2012, **22**, 24230.
19. S. C. Ray, A. Saha, N. R. Jana, R. Sarkar, *J. Phys. Chem. C*, 2009, **113**, 18546.
20. L. Cao, S. T. Yang, X. Wang, P. G. Luo, J. H. Liu, S. Sahu, *Theranostics*, 2012, **2**, 295.
21. M. Nurunnabi, Z. Khatun, K. M. Huh, S. Y. Park, Y. D. Lee, K. J. Cho, et al., *ACS Nano*, 2013, **7**, 6858.
22. SY Lim , Shen W, Gao Z, *Chem Soc Rev.* 2015, **44**, 362.
23. X. Chen, Q. Jin, L. Wu, C. Tung, X. Tang, *Angew. Chem. Int. Ed.* 2014, **53**, 12542.
24. Y. Zhu, X. Ji, C. Pan, Q. Sun, W. Song, L. Fang, Q. Chen, C. E. Banks, *Energy Environ. Sci.,* 2013, **6**, 3665.
25. D. Chao, C. Zhu, X. Xia, J. Liu, X. Zhang, J. Wang, P. Liang, J. Lin, H. Zhang, Z. Xiang Shen, H. J. Fan, *Nano Lett*., 2015, **15**, 565.
26. Y. Yang, X. Ji, M. Jing, H. Hou, Y. Zhu, L. Fang, X. Yang, Q. Chen, C. E. Banks, *J. Mater. Chem. A*, 2015, **3**, 5648.
27. L. Bhattacharjee, R. Manoharan, K. Mohanta, R. R. Bhattacharjee, *J. Mater. Chem. A,* 2015, **3**, 1580.
28. J. R. Lakowicz, *Principles of Fluorescence Spectroscopy*,1st edn., Plenum Press, New York, London, 1983.

29. F.Scholz (Ed), *Electroanalytical method-Guide to Experiments and Applications*, Spinger, DOI:10.1007/978-3-662-04757-6.
30. K. Morinaga, *Bull. Chem.Soc.* Japan 1956,**29**,793
31. H. Wang, A. Thiele, L. Pilon, *J. Phys. Chem. C*, 2013, **117**, 18286.
32. J. H. Engel, Y. Surendranath, A. Paul Alivisatos, *J. Am. Chem. Soc.* 2012, **134**, 13200.
33. M. Jankulovska, T. Berger, S. S. Wong, R. Gómez, T. Lana-Villarreal, *ChemPhysChem*, 2012, **13**, 3008.

Figures & Captions

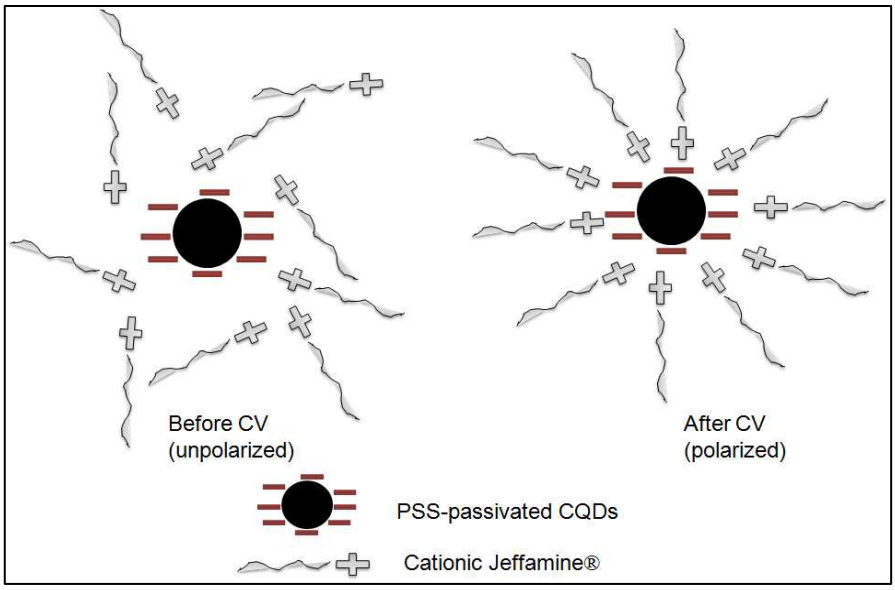

Scheme 1: Schematic representation of ordered and disordered structures of CQD-NIMs after and before CV.

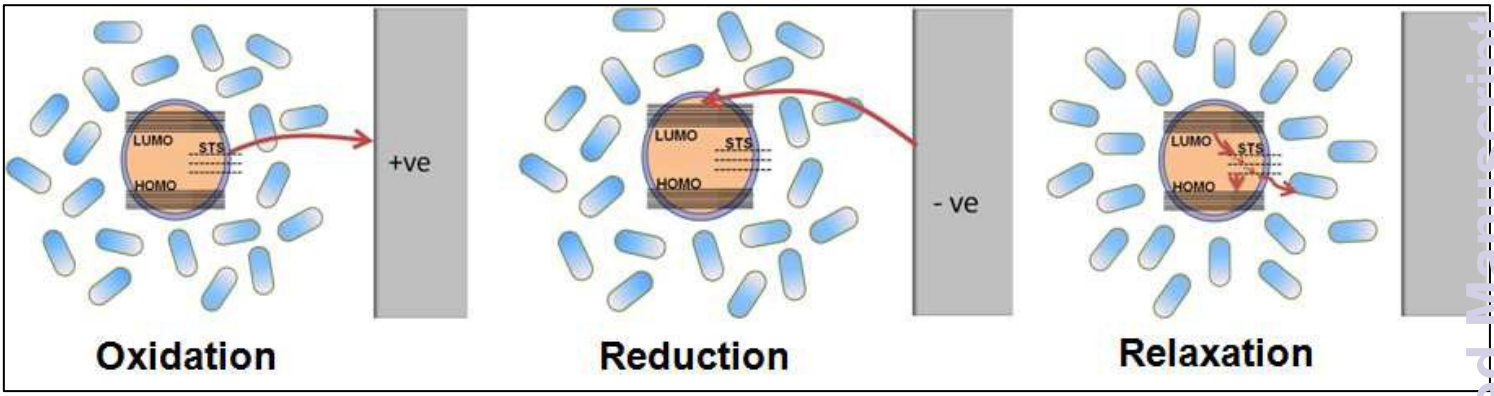

Scheme 2: Schematic representation of CV induced polarization of CQD-NIMs. The diagram shows different stages of electron transfer during CV cycle.

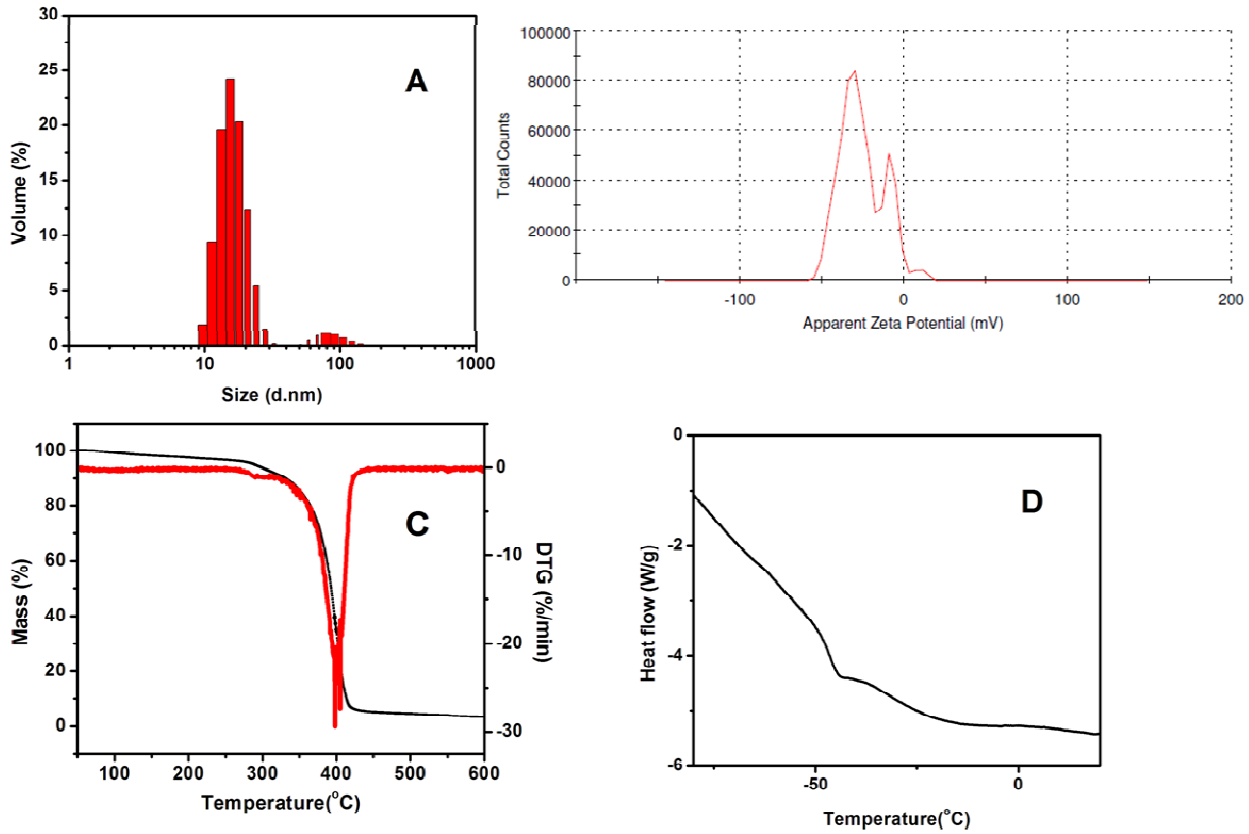

Fig. 1: (A) DLS data of CQD-NIMs volume-size distribution, (B) surface charge measurement through Zeta potential, (C) thermal stability (red and black correspond to DTG & TGA respectively) and (D) DSC data for glass transition temperature of CQD-NIMs.

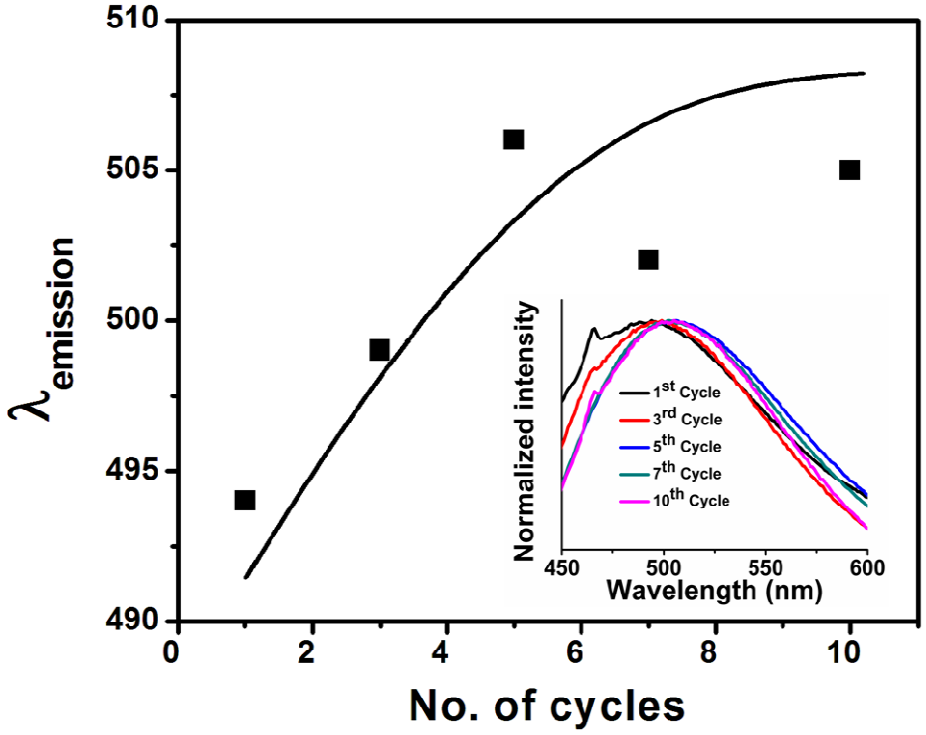

Fig. 2: Plot of λ_{em} of CQD-NIMs against number of CV cycles. Inset shows PL spectra as a function of CV cycles.

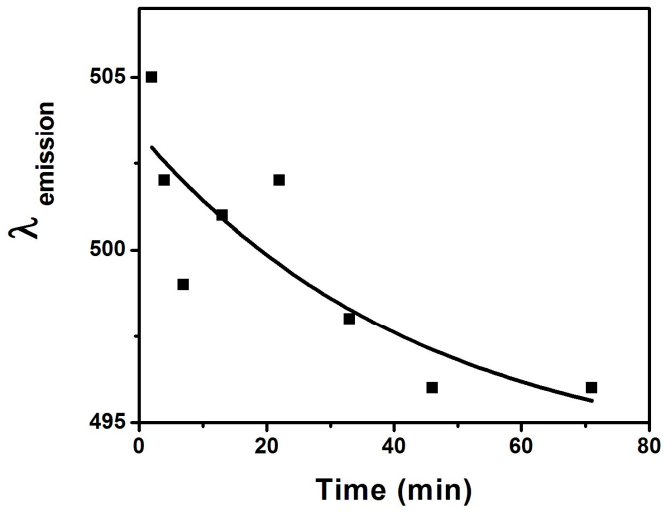

Fig. 3: Plot of λ_{em} of CQD-NIMs recorded after 10 CV cycles against relaxation time.

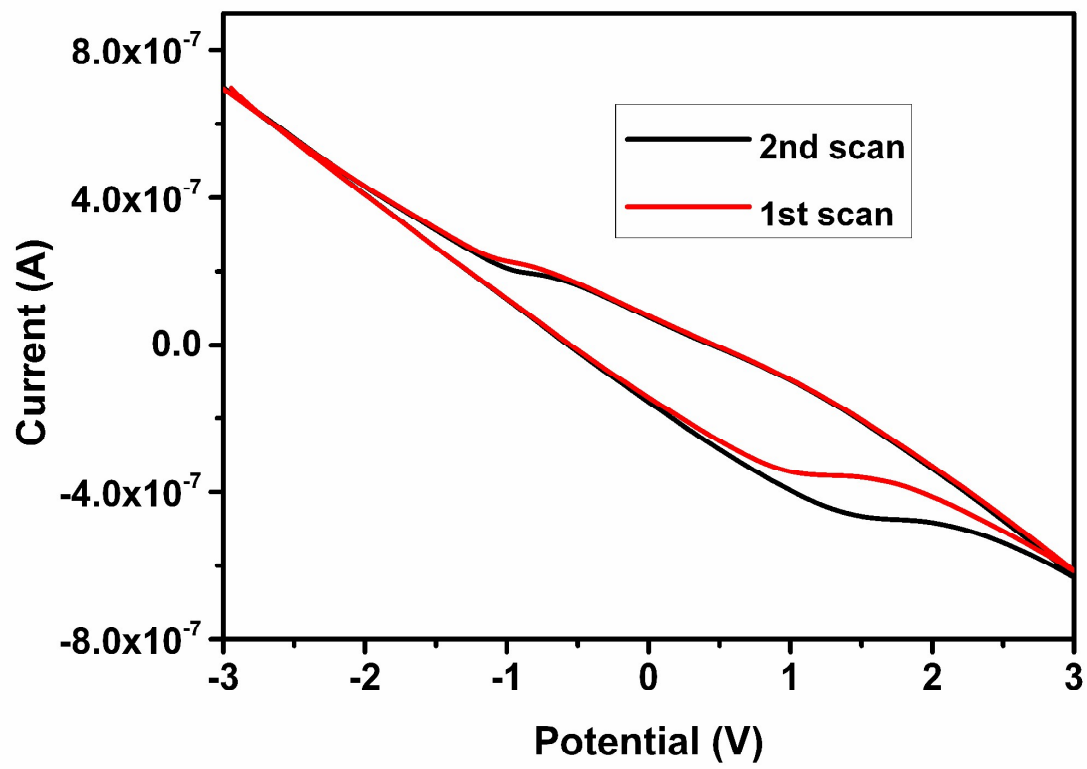

Fig. 4: CV of CQD-NIMs showing first & second cycles respectively.

TABLE OF CONTENT

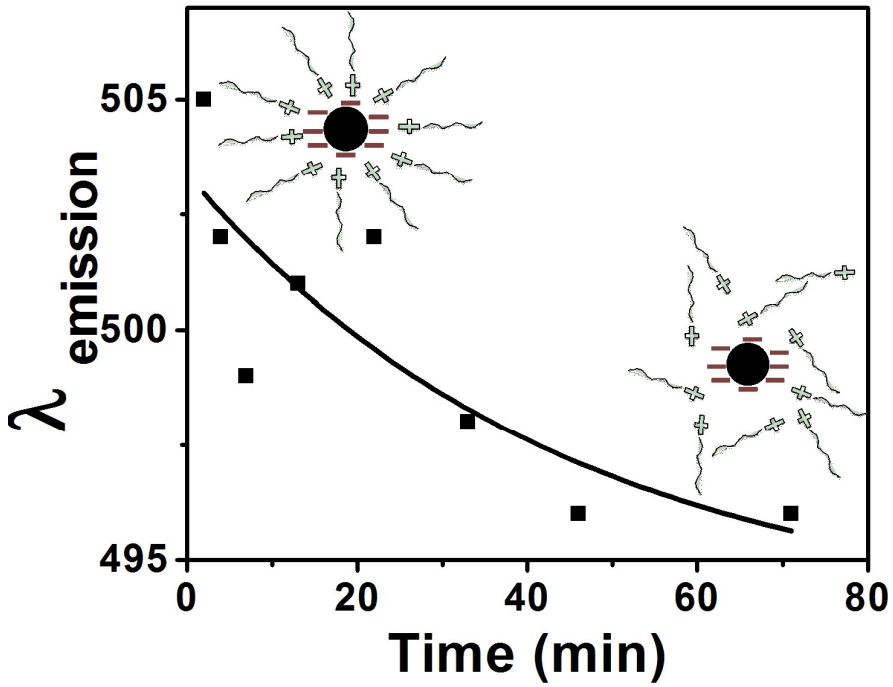

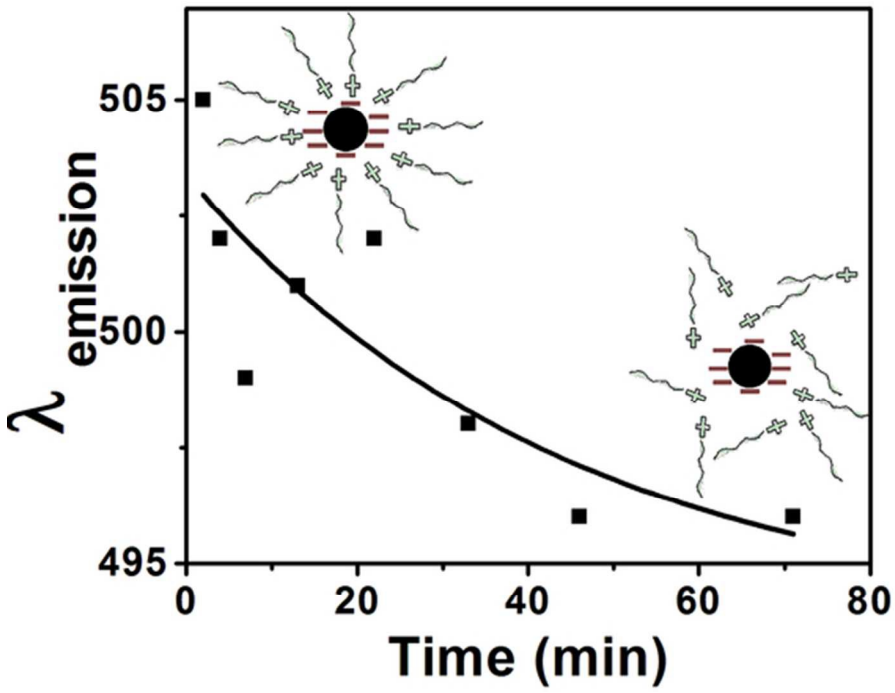

53x41mm (300 x 300 DPI)